Journal of Physics: Conference Series **510** (2014) 012030 doi:10.1088/1742-6596/510/1/012030

Effect of nitrogen impurity on the structural, mechanical and phonon properties of diamond from first-principle study

T.A. Ivanova[1,2], B.N. Mavrin[1]
[1] Institute of Spectroscopy of RAS, Fizicheskaya 5, Troitsk, Moscow 142190, Russia
[2] Technological Institute for Superhard and Novel Carbon Materials, Centralnaya 7a, Troitsk, Moscow 142190, Russia

E-mail: tas_88@mail.ru

Abstract. By means of density functional theory, we investigated physical properties of nitrogen-doped diamond and compared them with those of pure diamond. We showed that the nitrogen in substitution causes the strong lattice deformation near impurity, decreases elastic moduli, hardness and their anisotropy. We have confirmed experimental data that the face (111) is harder than face (100) in diamond. The nitrogen incorporation leads to an appearance of the resonant localized modes. The total and partial phonon densities of states, the mode localization, and the Raman and IR intensities in nitrogen-doped diamond were analyzed.

Introduction

The incorporation of impurities into the crystal leads to the change in the interatomic forces in the vicinity of the impurity and a relaxation not only adjacent, but also more distant atoms from the impurity [1]. As a result of this disturbance the crystal translational symmetry is broken and localized vibrational modes in the crystal phonon structure may appear. When the masses of the atoms of the impurity and the crystal are close, as it is in the case of diamond doped with nitrogen, one can expect only the appearance of resonant localized modes insides the phonon density of states of the pure crystal. The resonance modes hybridize with the lattice vibrations, and their theoretical study requires taking into account a large number of atoms in the crystal lattice with an impurity [2]. Ab-initio quantum mechanical methods are the most accurate for the investigation of the resonant vibrational states in crystals with an impurity, as well as for calculations of the physical properties of materials [3].

The nitrogen atom is the simplest and most dominant impurity in natural diamonds and especially in diamonds synthesized with a high pressure and high temperature or by CVD it mainly substitutes the carbon atoms at concentrations <1021 atoms/cm^3 (diamond type Ib). The neutral nitrogen in substitutional position is a donor impurity in diamond with an ionization energy of ~ 1.7 eV. Even at low concentrations, impurities and defects play an important role in the physical properties of diamond. The experimental [4] and theoretical [5,6] studies showed that the substitution of the carbon atoms by nitrogen leads to the elongation of the one of four N-C bonds, that causes local symmetry C_{3v} for a nitrogen atom. The reason for this nitrogen asymmetric position may be a Jahn-Teller instability [4] or the effects of local chemical bonds [7]. The previous ab initio calculations ([6] and refereces therein) concerned only the local structural distortion near nitrogen and electronic properties. The effect of nitrogen doping on the radial and bond angle distribution, phonon structure and mechanical properties are studied insufficiently in diamond. It is known that the IR absorption bands near 1130 [8] and 1344 [9] cm^{-1} appear in nitrogen-doped diamond and their intensity is gained with doping.

In this paper, using first-principles methods in the approximation of density functional theory, we study the structural parameters, elastic constants, elastic moduli, anisotropy of the elastic properties and hardness, the phonon density of states and localization of vibrational excitations in neutral-nitrogen-doped diamond, and these data are compared with those of the diamond without impurities.

2. Computational details

First-principles calculations were performed in the plane wave basis approximation, using the ABINIT package [10]. The FHI98PP pseudopotentials with GGA (PBE) exchange-correlation functional (from the ABINIT site) were used in the structural and elastic calculations and LDA Troulier-Martin pseudopotentials [10] in the Raman and IR calculations. We expect core electron effects to bonding at doping. Therefore, we implemented the effectively all-electron calculations to include these effects, using the projector augmented wave method. We used cutoff energy of 20 Ha for the wave functions and 60 Ha for the charge density. During the relaxation of nitrogen-doped structures and calculating the phonon density we used a 8x8x8 Monkhorst-Pack sampling [11] and 6x6x6 at the elastic constants calculations. The convergence of computations was controlled by parameter 10^{-10} Ha for total electron energy and less than 0.01 eV/Å for forces. The structure of the nitrogen-doped diamond was represented by 64-atom cubic supercell (the 2x2x2 repetition of 8-atom elementary diamond cell), where one carbon atom was replaced by nitrogen (NC_{63} cell). The distance between nitrogen atoms in the next supercells exceded 7 Å that allowed one not to consider an interaction between them. The supercell structure was relaxed with respect to the atom positions and lattice constants.

Table 1. Strains used to calculate elastic constants of cubic NC_{63}. Strains 2 and 3 are volume-conserving. B_2^V and B_2^δ are quadratic coefficients in the polynomial approximation of $\Delta E(V)$ and $\Delta E(\delta)$, respectively.

	Strains	Elastic constants
1	$\varepsilon_{xx} = \varepsilon_{yy} = \varepsilon_{zz} = \delta$	$c_{11} + 2c_{12} = 3B_2^V V_0$
2	$\varepsilon_{xx} = \delta,\ \varepsilon_{yy} = -\delta,\ \varepsilon_{zz} = \delta^2(1-\delta^2)^{-1}$	$c_{11} - c_{12} = B_2^\delta / V_0$
3	$\varepsilon_{xy} = \varepsilon_{yx} = \delta/2,\ \varepsilon_{zz} = \delta^2(4-\delta^2)^{-1}$	$c_{44} = 2B_2^\delta / V_0$

For the calculating of elastic constants c_{ij} we used the method of small strains ε_{ij} imposed to the equilibrium structure with the cell volume V_0, that leaded to the change of total electron energy E^{tot} after relaxation on size of elastic energy ΔE [12]:

$$\Delta E = E^{tot}(\varepsilon) - E^{tot}(0). \tag{1}$$

Cubic crystal has only three independent elastic constants of stiffness: c_{11}, c_{12} and c_{44} [13], which can be found using 3 types of strains with $\delta = -0.02 \div 0.02$ (Table 1). Elastic constants of compliance s_{ij} are associated with elastic constants of stiffness c_{ij} in cubic crystal by a ratio [13]:

$$\begin{aligned} s_{11} &= (c_{11} + c_{12}) / s_0, \\ s_{12} &= -c_{12} / s_0, \\ s_{44} &= 1 / c_{44}, \\ s_0 &= (c_{11} - c_{12})(c_{11} + 2c_{12}). \end{aligned} \tag{2}$$

In the isotropic approximation bulk modulus *B*, shear modulus *G*, Young's modulus *E* and Poisson's ratio σ are also defined by constants c_{ij} [14]:

$$\begin{aligned} B &= (c_{11} + 2c_{12})/3, \\ G &= (G_V + G_R)/2, \\ G_V &= (c_{11} - c_{12} + 3c_{44})/2, \\ G_R &= 5c_{44}(c_{11} - c_{12})/(4c_{44} + 3(c_{11} - c_{12})), \\ E &= 9BG/(3B + G), \\ \sigma &= (3B - 2G)/(6B + 2G). \end{aligned} \tag{3}$$

If we consider anisotropy of the cubic medium, the elastic moduli depend on direction [15]:

$$\begin{aligned} G_{lmn}^{-1} &= s_{44} - 4(s_{11} - s_{12} - s_{44}/2)\Phi, \\ E_{lmn}^{-1} &= s_{11} - 2(s_{11} - s_{12} - s_{44}/2)\Phi, \\ \sigma_{lmn} &= -\frac{s_{12} + (s_{11} - s_{12} - s_{44}/2)\Phi}{s_{11} - 2(s_{11} - s_{12} - s_{44}/2)\Phi}, \\ \Phi &= l^2m^2 + m^2n^2 + l^2n^2, \end{aligned} \tag{4}$$

where *l, m, n* are the directional cosines for direction [*lmn*]. The expression Φ in Eq. (4) is equal zero for the direction [100] and 1/3 for [111].

For the computation of phonon density of states in NC_{63} we used the direct method of calculating interatomic force constants. In this method first of all we calculate forces arising between atoms by shifting each atom from equilibrium in direction of axes x, y and z by ± 0.02 Å. For the sake of minimization our calculations we used symmetrical properties of crystal NC_{63}.

The force constants matrix with the dimension 192x192 were constructed by dividing derived forces by the atom shifts, then the standard crystal lattice theory was applied for the phonon density of states (PDOS) computation using program PHON [16]. We calculated total PDOS and partial PDOS which reproduces separately the nitrogen and carbon atoms contribution to the nitrogen and carbon atoms contribution to the PDOS. Partial PDOS was calculated also for different groups of carbon atoms equidistant from nitrogen atom. The PDOS and partial PDOS calculations were based upon the atomic displacements in the normal modes and the results were broadened by 0.3 cm^{-1}.

3. Results and discussions

3.1. Structural properties

After the relaxation nitrogen atom turned out to be displaced along the direction [111], occupying local position C_{3v} and retaining the fourfold coordination, as it was showed in previous works [5,6]. In the NC_{63} cell the carbon tetrahedrons adjacent to the nitrogen has been deformed. For the detailed investigation of local structure we calculated the radial and bond angle distributions in crystal NC_{63}.

The distribution of interatomic bondlengths in relaxed NC_{63} crystal cell (Figure 1) shows that one N-C_1 bond has the length about 2 Å, while three others N-C_3 less than 1.5 Å. Most of the others C-C bonds length are groupped near 1.54 Å that is near the C-C length in pure diamond. But three C_1-C_2 bonds adjacent to the lengthy bond C_1-N become shorter than 1.5 Å. The lattice constant of cubic crystal NC_{63} increases slightly in comparison with the doubled lattice constant of the diamond cell (7.159 and 7.09 Å, correspondingly). The lattice expansion at substitutional nitrogen doping was observed in experiments [17,18].

The bond angle distribution, that is the angles distribution between adjacent bonds for every atom shows (Figure 2) that average angle between bonds is close to the tetrahedral angle $\theta = 109.47^{\circ}$. Some deviations from θ are observed only for atoms, bonded to the nitrogen atom and to the nearest carbon

atoms. From the radial (Figure1) and bond angle (Figure 2) distributions we can conclude that the substitutional nitrogen atom in diamond brought only local distortions in the diamond lattice.

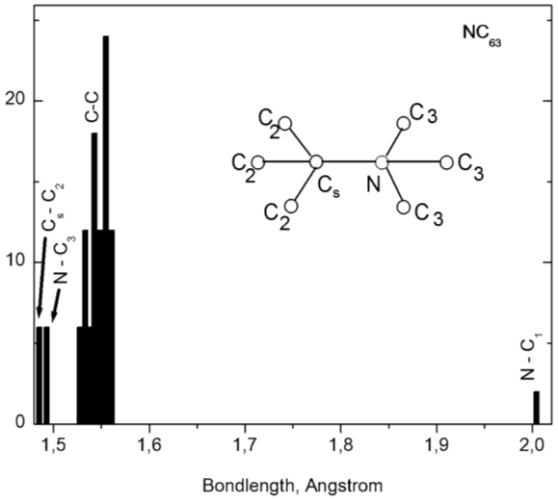

Figure 1 The distribution of bonds depending on bondlengths in a relaxed crystal NC_{63}. Insert: a schematic arrangement of the nearest carbon atoms near nitrogen.

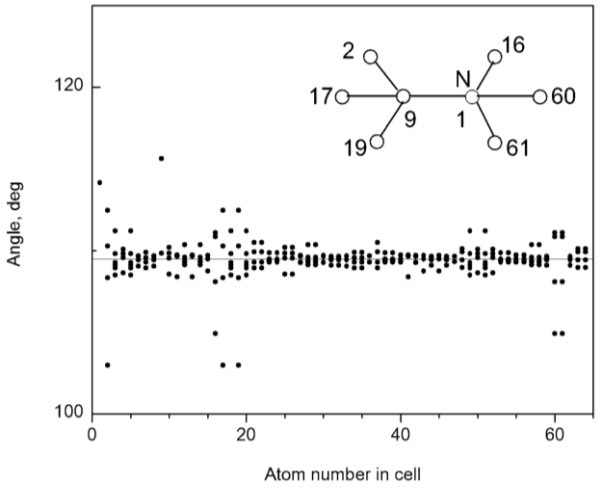

Figure 2 The bond angle distribution depending on the distance from the origin of the NC_{63} cell.

3.2. Mechanical properties

The calculated dependences $\Delta E^{tot}(V)$ and $\Delta E(\delta)$ allowed us to find the bulk modulus B and elastic constants c_{11}, c_{12} and c_{44} for diamond and crystal NC_{63}. The calculated elastic constants and the elastic moduli in the isotropic approximation for diamond and crystal NC_{63} are presented in Table 2. The theoretical values for diamond are compared with experimental data [19-21]. The elastic constants and moduli of crystal NC_{63} were less than in diamond, that point to the lower stiffness and greater compressibility of nitrogen-doped diamond.

Table 2. Elastic constants and moduli in the isotropic approximation (in GPa) for diamond and NC_{63}.

		c_{11}	c_{12}	c_{44}	B	G	E	σ	A	k
Diamond	Calc.	1022	151	595	467	543	1174	0.081	1.37	1.16
	Exp.	1078	126	577	444	535	-	-	-	-
NC_{63}	Calc.	1026	134	532	432	496	1076	0.084	1.19	1.15

The distinction between the diamond and crystal NC_{63} elastic properties is clearly visible using a graphical representation of a quasilinear states equation [22]:

$$\begin{aligned} \mathrm{Ln}[\,px^2/(3(1-x))] = \mathrm{Ln}Y = \mathrm{Ln}B + A_0(1-x), \\ x = (V/V_0)^{1/3},\ A_0 = 3(B^{'}-1)/2, \end{aligned} \tag{5}$$

where p is the pressure and $B' = dB/dp$. The pressure p was obtained after the cell relaxation at a given x. Figure 3 shows that the dependences LnY are almost linear for both crystals. As far as LnY = LnB when x = 1, it allows us to find bulk moduli (Table 2). The value LnY at x = 1 for a crystal NC_{63} has less value than for the diamond (Figure 3) and the bulk modulus is accordingly smaller. The inclination of the linear dependence LnY that is the coefficient A_0 in the Eq. (5), is a little bit more for NC_{63}, than for diamond, therefore the coefficient B' is also larger (3.85 and 3.70, correspondingly).

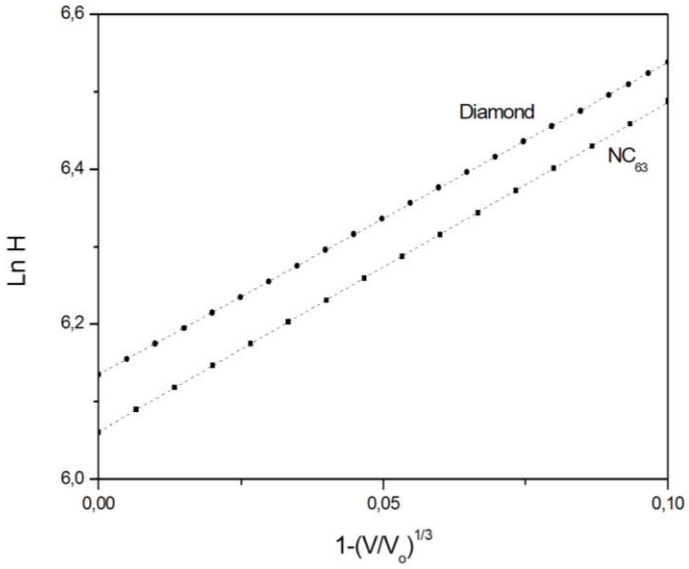

Figure 3 The quasilinear equation of states for diamond and NC_{63}. The parameter $1-(V/V_0)^{1/3}$ corresponds to a range of pressure of 0-250 GPA.

The material elasticity can be characterized by Pug's parameter [23]: $k = G/B$. Since this parameter is much greater than 0.5 in both crystals (Table 2), materials are brittle, although the parameter k in the crystal NC_{63} is smaller. The higher NC_{63} elasticity is confirmed by greater value of Poisson's ratio σ, which shows the change in the transversal dimensions at the longitudinal elongation.

The elastic anisotropy of isotropic medium is usually estimated by Zener factor [24] $A = 2c_{44}(c_{11} - c_{12})^{-1}$. Table 2 shows that the factor A decreases in the crystal NC_{63} compared to diamond, that means that nitrogen-doped diamond becomes more isotropic.

A more detailed analysis of the elastic properties anisotropy can be carried out with the help of Eq. (4) and the results are given in Table 3. Anisotropic elastic moduli G_{100} and G_{111} (Table 3), exceed the isotropic value of G (Table 2), that may indicate that isotropic approximation is insufficient for the study of elastic properties in both diamond and crystal NC_{63}. The anisotropy of elastic properties , i.e. relations G_{111}/ G_{100} and E_{111}/ E_{100} are less in crystal NC_{63} than in diamond that confirms smaller anisotropy of elastic properties in crystal NC_{63} in comparison with diamond.

Table 3. Elastic constants of compliance s_{ij} (in 10^{-4} GPa^{-1}) and anisotropic elastic moduli (in GPa) for diamond and NC_{63}.

	s_{11}	s_{11}	s_{11}	G_{100}	G_{111}	E_{100}	E_{111}	σ_{100}	σ_{111}
Diamond	10.172	-1.309	16.806	595	787	1017	1231	0.128	0.035
NC_{63}	10.054	-1.161	18.801	532	610	1005	1131	0.115	0.063

Nowadays the hardness calculation is based on semi-empirical models ([25] and references there), from which we have used a model that assumes a correlation between the hardness H and the elastic moduli [25,26]:

$$H = 2(G^3 / B^2)^{0.585} - 3 \quad (6)$$

This model has been satisfactorily described the hardness of various materials [25]. If in Eq. (6) we use the value G in the isotropic approximation (Table 2), we find that hardness is 92 GPa for diamond and 86 GPa for crystal NC_{63}. Thus the hardness of nitrogen-doped diamond decreases. If we use the anisotropic elastic moduli values (Table 3), we find that the H_{100} = 108 GPa and H_{111} = 152 GPa for diamond and 98 and 132 GPa, correspondingly, for the crystal NC_{63}. The calculated hardness anisotropy in diamond correlates with the experimental data [27] and suggests that hardness of the face (111) is much larger than the face (100) hardness. The ratio $H_{111/}$ H_{100} in diamond is higher than in the crystal NC_{63}, i.e. the hardness of nitrogen-doped diamond is not only reduced, but also have tendency of reduction the anisotropy.

3.3. Phonon density states and localization

In the phonon density of states (PDOS) of the Crystal NC_{63} (Figure 4), that it is similar to thediamond PDOS, the most intense band near 1220 cm^{-1} is downshifted by 40 cm^{-1} and all the bands are much wider. Since the band at 1220 cm^{-1} is caused by the contribution of optical modes in diamond, its low-frequency shift in NC_{63} indicates that the interatomic interaction between the carbon atoms weakens in nitrogen-doped diamond.

To investigate the nitrogen atom contribution and local carbon atoms contribution in the PDOS, we calculated the partial contributions of atoms in NC_{63} cell (Figure 5). The inset in Figure 5 shows one eighth cell. The carbon atom 6 is the furthest from the nitrogen atom 1. The nitrogen atom forms with the carbon atom 3 a long bond (~ 2 Å), and a short bond with the atom 2. The nitrogen atom contribution (PDOS1 in Figure 5) is concentrated mainly near 800 and 1100 $cm^{-1.}$ The majority of carbon atoms contribution is maximum at 1220 cm^{-1} (PDOS2, PDOS4-PDOS6), except the atom 3 contribution, which is removed from the nitrogen atom and forms three short bonds with nearest carbon atoms, that causes the appearance of band at 1329 cm^{-1} (PDOS3). Thus, the vibrations with the nitrogen participation have frequencies within the diamond PDOS, i.e. the carbon atom replacement by nitrogen leads only to the emergence of the impurity resonant localized modes in the diamond phonon structure.

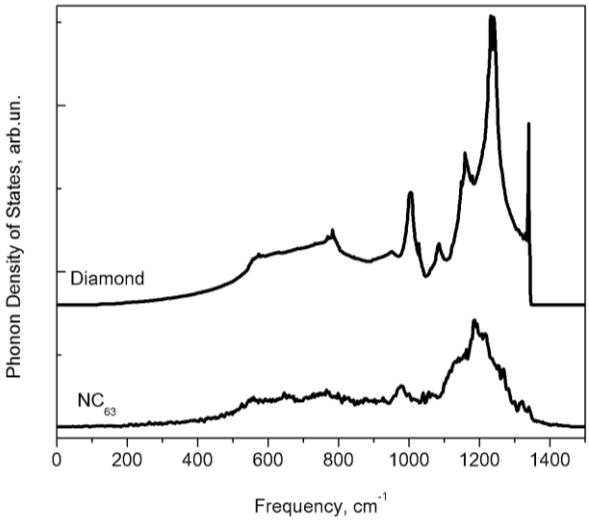

Figure 4 The total PDOS in diamond and $NC_{63.}$

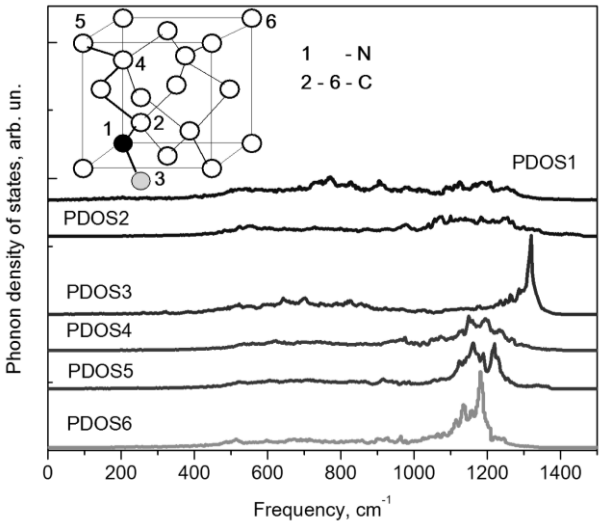

Figure 5 The partial PDOS of atoms in NC_{63}: PDOS1 is the partial PDOS of nitrogen, PDOS2-PDOS6 are the partial PDOS of carbon atoms 2-6 that are shown in inset. Inset: one eighth cell NC_{63}.

As far as in optical experiments (Raman scattering and IR absorption) the spectrum intensity is determined mainly by modes in the centre of Brillouin zone, we investigated PDOS of modes with $\boldsymbol{q}$ = 0. In particular, the local vibrational density of nitrogen atom (LPDOS) in NC_{63} at $\boldsymbol{q}$ = 0 can be found as [28]

$$LPDOS(\omega) = g(\omega)\left|\boldsymbol{e}(N,\omega)\right|^2, \quad (7)$$

where $g(\omega)$ is the total PDOS and $\boldsymbol{e}(N, \omega)$ is the nitrogen displacement vector in the normalized eigenvector of the mode at the ω frequency at $\boldsymbol{q} = 0$. Figure 6 shows that intensity maxima in LPDOS are in the same frequency region as in the partial PDOS1 (Figure 5), calculated for the contribution of the nitrogen atom to PDOS from all Brillouin zone. The displacements of the nitrogen and the nearest carbon atoms are shown in Figure 7 (inset) for the mode 800 cm-1 with the intensive LPDOS. It is seen that in this mode the atom of nitrogen moves in an antiphase with the closest atoms of carbon. The displacements amplitudes for the other carbon atoms in this mode are much smaller.

The eigenvectors at $\boldsymbol{q} = 0$ allowed us to investigate the mode localization in NC_{63}. For this one often calculate the inverse participation ratio (*IPR*), being the next sum over all cell atoms *n* [29]:

$$IPR(\omega) = \Sigma[\boldsymbol{e}_i(N,\omega)\cdot\boldsymbol{e}_i(N,\omega)]^2, \quad (8)$$

$IPR(\omega) = 1$ for a fully localized mode and $IPR(\omega) = 1/n$ for delocalized modes. In Figure 7 the majority of the modes have $IPR(\omega) \approx 2/n$ and the most localized are acoustic mode at 330 cm-1 and the optical mode at 1300 cm-1 with $IPR(\omega) \approx 6/n$. The modes at 600, 800 and 1100 cm^{-1} with the greatest nitrogen participation also have values ($IPR(\omega) \approx 4/n$), that exceed IPR of the majority of modes. Hence, impurity modes in nitrogen-doped diamond are weakly localized because of the strong hybridization with lattice modes.

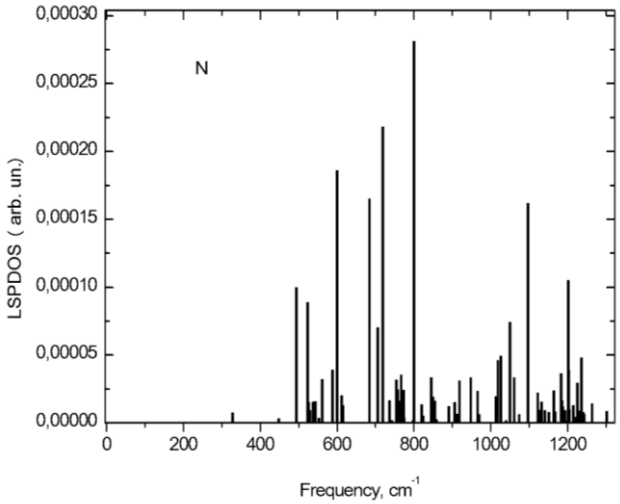

Figure 6 The local vibrational density of nitrogen in NC_{63} at $\boldsymbol{q} = 0$.

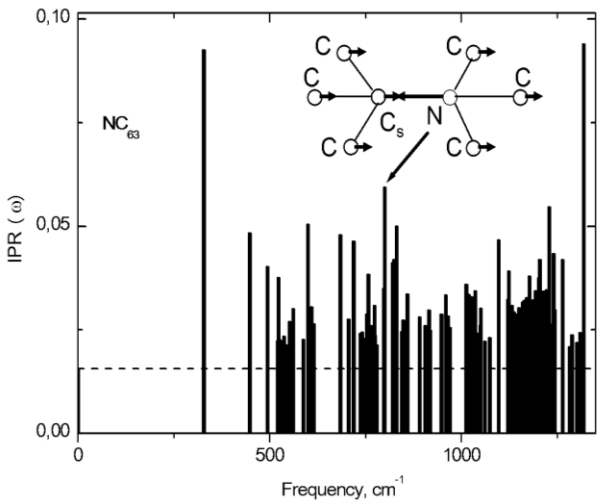

Figure 7 The inverse participation ratio IPR for modes in NC_{63} depending on frequency. Inset: displacements of the nitrogen and the nearest carbon atoms in mode at 800 cm^{-1}.

3.4. Raman and IR spectra

We have calculated the Raman and IR spectra for the crystal NC_{63} in LDA approximation. Previously the relaxation with this pseudo-potential was carried out. The nonresonant Raman spectrum intensity is proportional to the differential scattering cross section, which is determined by the square of the components in Raman tensor. The Raman tensor components were calculated in the Placzek approximation [30]. In the scattering geometry which is defined by tensor component α_{zz}, more intensive are the bands that are below 900 cm^{-1}, whereas in the crossed geometry α_{xz} intense bands are concentrated near 1300 cm^{-1} (Figure 8). The nitrogen atom contribution is maximum in the intensity of bands marked by asterisks in Figure 8.

The infrared absorption intensity is proportional to the square of the tensor components of the effective Born charge and eigenvectors [31]. The Born effective charge tensor was determined by the derivative of the forces acting upon the atom to the applied electric field [32]. The nitrogen atom has the largest contribution to the IR intensity for the bands near 500 and 1120 cm^{-1} (Figure 8). Previously [8] the band near 1130 cm^{-1} was observed in the IR spectrum and its intensity depended on the nitrogen concentration. In the calculated IR spectrum are seen the intense bands in the 1310-1330 cm^{-1} region with a small nitrogen contribution. Their intensity is mainly caused by the shortened C_2-C_1 bonds adjacent to the lengthy bond C_1-N (Figs. 1 and 5). These bands may be assigned to the local vibrational modes of carbons near nitrogen. If to consider that frequencies are underestimated in our calculations by ~ 1 %, it is possible assume that the observed IR band at 1344 cm^{-1} [9] is one of these modes.

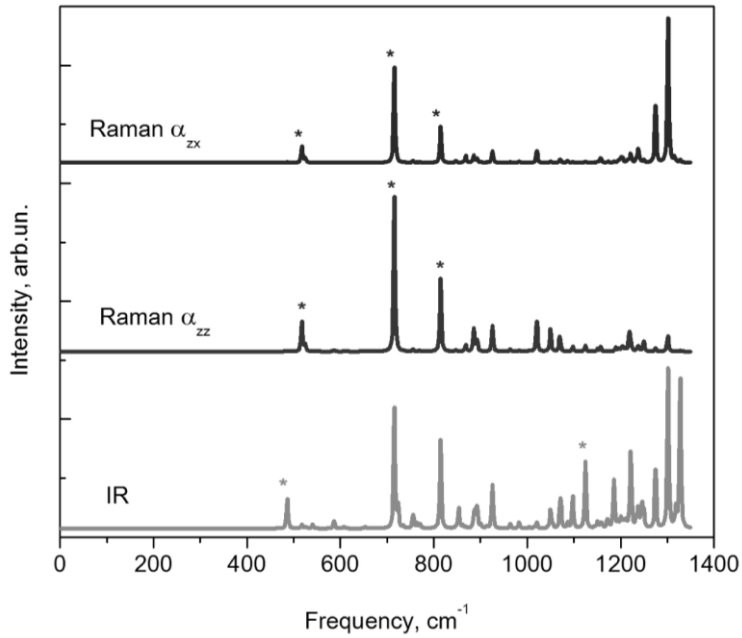

Figure 8 The Raman (α_{zz}, α_{xz}) and IR intensities of modes in NC_{63}. The modes with the greatest contribution of nitrogen are designated by an asterisk.

4. Conclusion

Using first-principles calculations we investigated the structural, mechanical and phonon properties of the diamond doped with nitrogen and compared them with the properties of pure diamond. The calculated results for the pure diamond are in good agreement with experimental data and other ab-initio calculations.

When nitrogen is in a substitution position, the lattice constant of diamond slightly increases, the elastic constants and moduli reduces. In nitrogen-doped diamond the elastic anisotropy decreases, the crystal becomes less brittle. The investigation of elastic anisotropy has shown that isotropic approximation is nonsufficient for the study of elastic properties in both pure and nitrogen-doped diamond. The hardness of nitrogen-doped diamond decreases. The calculated hardness anisotropy of diamond confirmed the experimental data that the hardness of the face (111) is much higher than the hardness of the face (100). The nitrogen doping tends to reduce the hardness anisotropy.

The PDOS bands of diamond are shifted down at nitrogen doping that testifies to weakening of interatomic interaction in nitrogen-doped diamond. The study of partial PDOS has shown that the nitrogen contribution is seen only within the PDOS of pure diamond that causes an appearance of resonant localized modes. The modes with the greatest nitrogen participation are more localized in

comparison with the majority modes. Unlike pure diamond the Raman tensor component α_{zz} is not equal to zero. The crossed component α_{xz}, as expected, is largest for modes near 1300 cm^{-1}.

Our calculations are consistent with the following experimental data: a C_{3v} local symmetry of nitrogen site in diamond, a lattice expansion in nitrogen-doped diamond, the frequencies of localized modes of carbons near nitrogen have the highest value in comparison to other modes, the noticeable contribution of nitrogen in IR intensity near 1100 cm^{-1}, the calculated elastic constants in diamond, hardness of the (111) face in diamond is higher than that of the (100) face.

Results of the carried-out calculations showed that, as masses of nitrogen and carbon differ a little, local modes of nitrogen have a resonant character, they are strongly hybridized with the diamond modes and they become poorly localized. On the other hand, a lattice distortion by nitrogen has the local character in nitrogen-doped diamond.

Acknowledgements
This work was supported by program "Physics of New Materials and Structures" of OFN RAS. The calculations were carried out at Interdepartmental Supercomputer Centre of RAS.

References
[1] Maradudin A A 1966 *Solid State Physics* **18** 273
[2] Petzke K 1999 *Phys. Rev.* B **60** 12726
[3] Baroni S, de Gironcoli S, Corso A D and Giannozzi P 2001 *Rev. Mod. Phys.* **73** 515
[4] Smith W V, Sorokin P P, Gelles I L and Lasher G J 1959 *Phys. Rev.* **115** 1546
[5] Kajihara S A, Antonelli A, Bernholc J and Car R 1991 *Phys. Rev. Lett.* **66** 2010
[6] Lombardi E B, Mainwood A, Osuch K and Reynhardt E C 2003 *J. Phys.: Condens. Matter* **15** 3135
[7] Bachelet G B, Baraff G A, and Shluter M 1981 *Phys. Rev.* B **24** 4736
[8] Collins A T 1980 *J. Phys.* C **13** 2641
[9] Collins A T and Woods G S 1982 *Phil. Mag*. **46** 77
[10] www.abinit.org
[11] Monkhorst H J and Pack J D 1976 *Phys. Rev.* B **13** 5188
[12] Wu Z, Chen X-J, Struzhkin V V, and Cohen R E 2005 *Phys. Rev* B **71** 214103
[13] Nye J F 1985, *Physical Properties of Crystals: Their Representation by Tensors and Matrices* Oxford Univ. Press.
[14] Wu Z-j, Zhao E-j, Xiang H-p, Hao X-f, Liu X-j and Meng J 2007 *Phys. Rev.* B **76** 054115
[15] Date E H F and Andrews K W 1969 *Brit. J. Appl. Phys. (J. Phys. D)* **2** Ser. 2 1373
[16] Alfè D 2009 *Computer Physics Communications* **180** 2622
[17] Kiflavi I, Mayer A E, Spear P M, Van Wyk J A and Woods GS 1994 *Phil. Mag.* B **69** 1141
[18] Boyd S R, Kiflavi I andWoods G S 1994 *Phil. Mag.* B **69** 1149
[19] McSkimin H J and Andreath J P 1972 *J. Appl. Phys.* **43** 2944
[20] Grimsditch M H and Ramdas A K 1975 *Phys. Rev.* B **11** 3139
[21] Zouboulis E S, Grimsditch M, Ramdas A K and Rodriguez S 1998 *Phys. Rev.* B **57** 2889
[22] Francisco E, Blanco M A and Sanjurio G 2001 *Phys. Rev.* B **63** 094107
[23] Pugh S F 1954 *Philos. Mag.* **45** 823
[24] Zener C 1948 *Elasticity and anelasticity of metals*, Chicago, University of Chicago Press
[25] Chen X-Q, Niu H, Li D and Li Y 2011 *arXiv*: 1102.4063v1 [cond-mat.mtrl-sci]
[26] Niu H, Wei P, Sun Y, Chen X-Q, Franchini C, Li D and Li Y 2011 *Appl. Phys. Lett*. **99** 031901
[27] Blank V, Popov M, Lvova N, Gogolinsky K and Reshetov V 1997 *J. Mater. Res.* **12** 3109
[28] Fultz B 2010 *Progress in Materials Science* **55** 247
[29] Atta-Fynn R and Biswas P 2009 *J. Phys.: Condens. Matter*. **21** 265801
[30] Sosso G S, Caravati S, Gatti C, Assoni S and Bernasconi M 2009 *J. Phys.: Condens. Matter* **21** 245401
[31] Giustino F and Pasquarello A 2008 *Phys. Rev.* B **78** 075307
[32] Gonze X and LeeC 1997 *Phys. Rev.* B **55** 10355